# Atomic data and opacities computations for kilonovae at University of Mons

Patrick Palmeri

ASOS15 Nice

UMONS

fnrs
LA LIBERTÉ DE CHERCHER

EOS
THE EXCELLENCE
OF SCIENCE

# Belgian team

UMONS

- Pascal QUINET
- Patrick PALMERI
- Jérôme DEPRINCE
- Lucas MAISON
- Helena CARVAJAL GALLEGO
- Sirine BEN NASR

ULB

- Stéphane GORIELY
- Gururaj WAGLE
- Michel GODEFROID
- Sophie VAN ECK

# Outlines

- Astrophysical context
- Methods
- Results
- Conclusion & Prospects

# Astrophysical context

GW170817 event:

- Detection of gravitational waves from neutron star merger for the first time on August 17, 2007 (Abbott+, 2017)

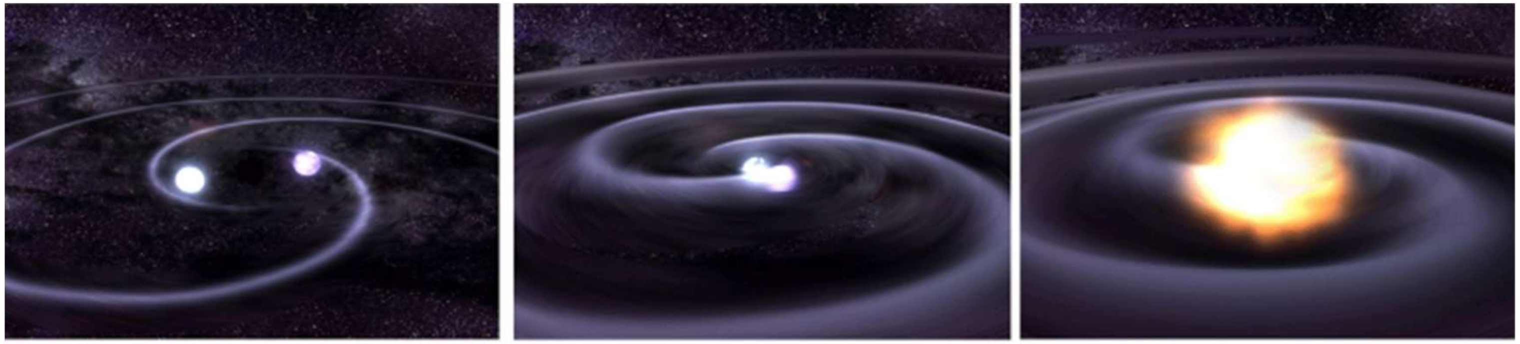

Evolving neutron star binary system (NASA/CXC/GSFC/T. Strohmayer)

- Also produces electromagnetic signal powered by the ejection of hot and radioactive matter: kilonova (KN)

# Astrophysical context

- Heavy r-processed elements (Z>26) are abundant in KN.
- Lanthanides & actinides dominate the KN opacity due to their large spectral density (open f-subshell) and abundances.

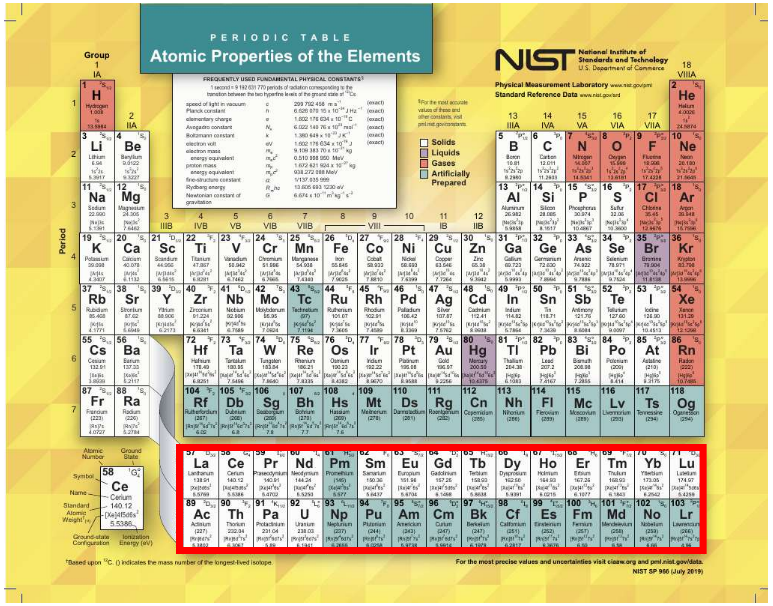


Periodic Table (NIST)

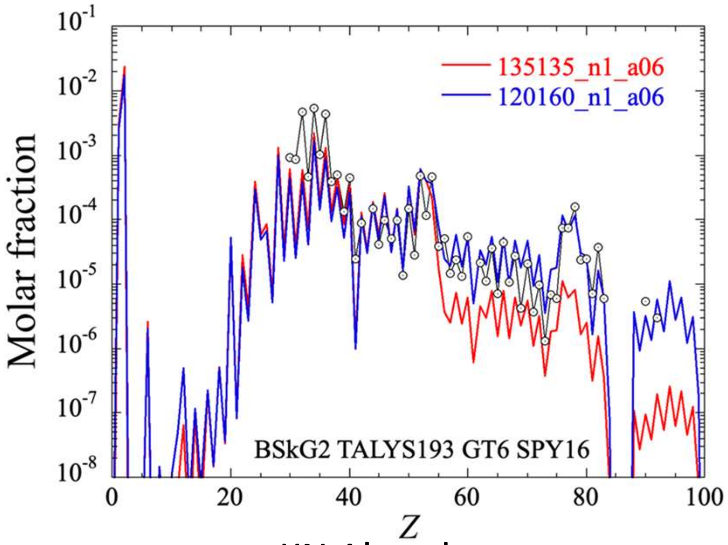


KN Abundances
(Goriely & Just, private communication)

# Astrophysical context

Photospheric phase from 1 day to ~1 week after NS merger (LTE)

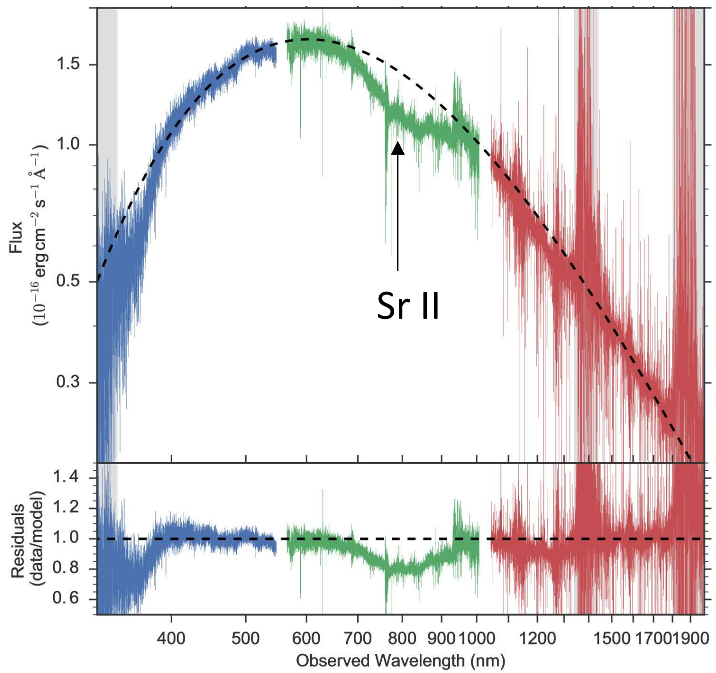


AT2017gfo (+1.5 d) (Watson+,2019)

$10^{-17}$ (g cm$^{-3}$) < ρ < $10^{-13}$ (g cm$^{-3}$)

1000 K < T < 10 000 K

Only charge states I - IV

E1 lines in absorption (Sr II)

Structure data only

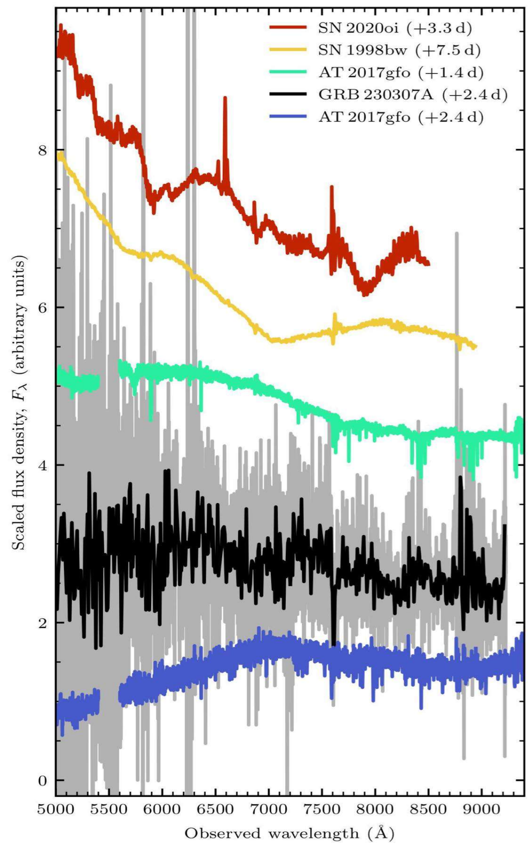


AT2023vfi (GRB230307A) (Levan+,2023)

# Astrophysical context

Nebular phase from ~1 week after NS merger (NLTE)

$\rho < 10^{-17}$ (g cm$^{-3}$)

T < 1000 K

Only charge states I - III

Forbidden lines in emission

Structure & collisional data

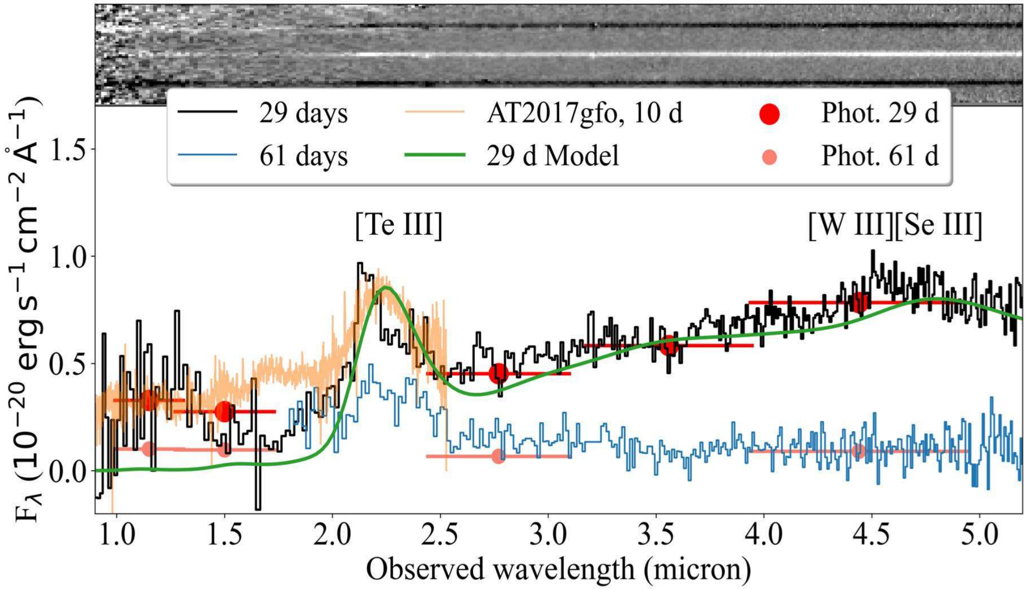


JWST/NIRSpec AT2023vfi (GRB230307A) KN spectra (Levan+, 2023)

# Methods: atomic structure

**Multi-Configuration Dirac-Hartree-Fock (GRASP) (Froese-Fischer+,2019):**

Relativistic method based on the Dirac equation

Introduction of correlation effects in an explicit way

QED corrections added in a perturbative way

Valence-valence + core-valence + core-core model: allowing SD excitations from spectroscopic orbitals towards some correlation orbitals

Semi-empirical correction: fine-tuning (Li+, 2023)

# Methods: atomic structure

**Pseudo-relativistic Hartree-Fock (HFR) (Cowan's code) (Cowan, 1981):**

Based on the Schrodinger equation

Introduction of valence correlation effects in an explicit way

Relativistic corrections added in a perturbative way

Orbitals obtained for each configuration by solving the HF equations

Codes actually developped by Cowan (1981) for opacity computation purposes

Semi-empirical adjustments can be done for detailed spectral modeling

# Methods: atomic structure

- MCDHF & HFR for computing forbidden lines
- HFR atomic data to calculate opacities

Advantages of HFR method:

- Calculation is relatively quick, even for a large number of configurations considered (large number of transitions)
- States from all the configurations are optimized

→ Suitable for computing physical quantities as opacity which requires to consider a large number of transitions

# Methods: collisional properties

Distorted Wave (DW):

- Channel coupling neglected but resonances can be added perturbatively
- Fast and efficient
- Multi-Configuration Breit-Pauli code AUTOSTRUCTURE (Badnell, 2011)

Plane-Wave Born (PWB):

- Neglects interaction between the free electron and the target ion
- Very basic but very fast
- Implemented in the Cowan's code,  targets from structure computations ready to be used

# Methods: expansion opacity

Expansion formalism:

$$\kappa_{exp}^{bb}(\lambda) = \frac{1}{\rho c t} \sum_l \frac{\lambda_l}{\Delta\lambda} (1 - e^{-\tau_l})$$

with the Sobolev optical depth:

$$\tau_l = \frac{\pi e^2}{m_e c} t n_l \lambda_l f_l$$

→ Radiative transition wavelength $\lambda_l$, oscillator strength $f_l$ and level population $n_l$ are needed

LTE → $n_l$ determined using Boltzmann and Saha equations

# Methods: line-binned opacity

$$\kappa_{bin}^{bb} = \frac{1}{\Delta\nu}\frac{\pi e^2}{\rho m_e c}\sum_l n_l f_l$$

Comparison between line-binned and expansion opacity:

$$\kappa_{g,n}^{bb} = \frac{1}{\rho_n c t_n}\frac{1}{\Delta\lambda_g}\sum_{l\in\Delta\lambda_g}\begin{cases}\lambda_l\tau_l & \text{for binned}\\ \lambda_l(1-e^{-\tau_l}) & \text{for expansion}\end{cases}$$

(Fontes+, 2020)

Advantages line-binned opacities vs expansion opacities:

- Does not depend on expansion time
- Proportionnal to $\tau$ , so to $n$, so to the abundances

→ Can be tabulated and used for different NSM models

# Results: LTE

**Kilonova ejecta opacity inferred from new large-scale HFR atomic calculations in all elements between Ca ($Z = 20$) and Lr ($Z = 103$)★**

J. Deprince[1,2], G. Wagle[2], S. Ben Nasr[1], H. Carvajal Gallego[1], M. Godefroid[3], S. Goriely[2], O. Just[4,5], P. Palmeri[1], P. Quinet[1,6], and S. Van Eck[2]

Astronomy & Astrophysics **696**, A32 (2025)

Creation of an atomic and opacity database:
HFR Atomic Database and Opacity Tables for Kilonovae from Mons and Brussels Universities
DOI 10.5281/zenodo.14724537

LTE opacities implemented in the KN RT modeling code SuperNu

# Results: LTE

Comparison with Tanaka+(2020), HULLAC v1, 26 ≤ Z ≤ 89 (no actinide)
Planck expansion opacities

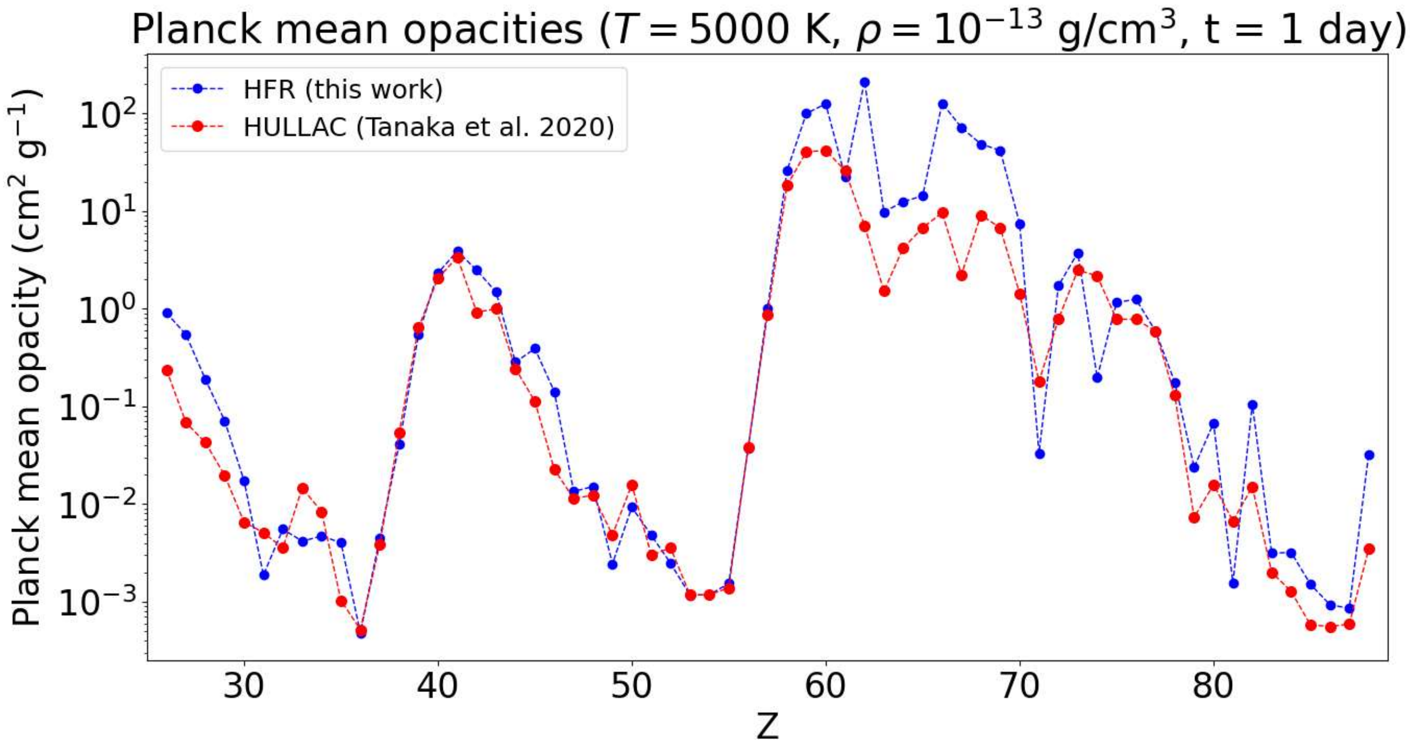

# Results: LTE

Comparison with Fontes+(2020 &2023), lanthanides & actinides
Planck line-binned opacities

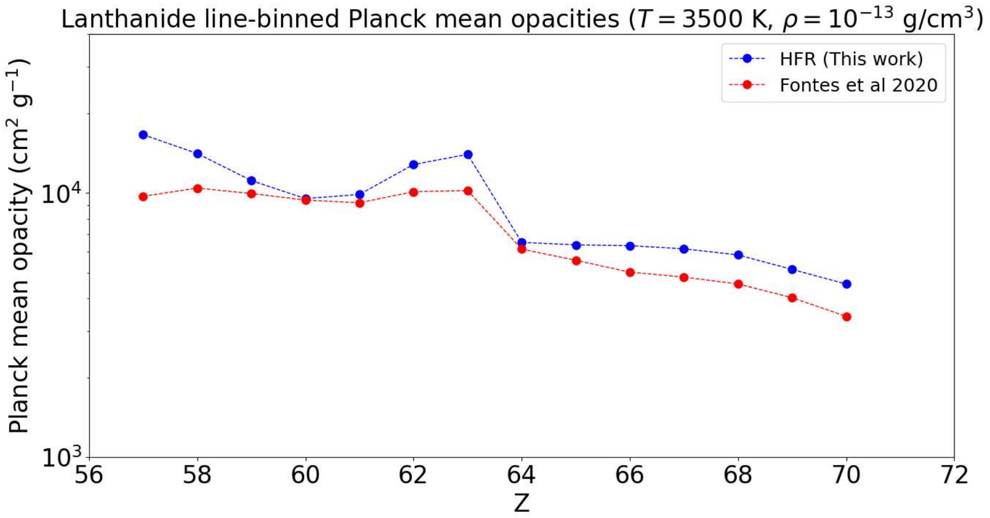


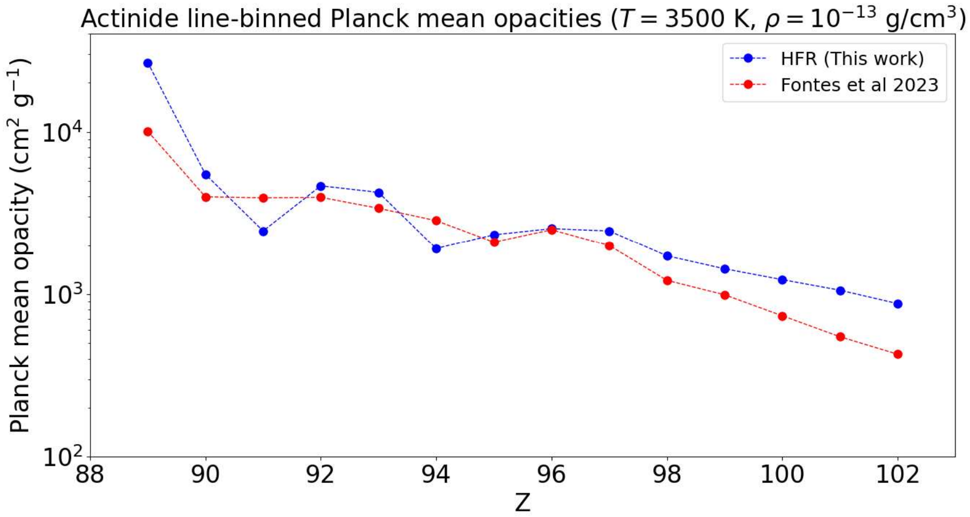

# Results: LTE

Kilonova ejecta total opacity

NSM model (Just+, 2023) at +3.5d, $T$= 6000 K, $\rho$ = $10^{-13}$ g cm$^{-3}$

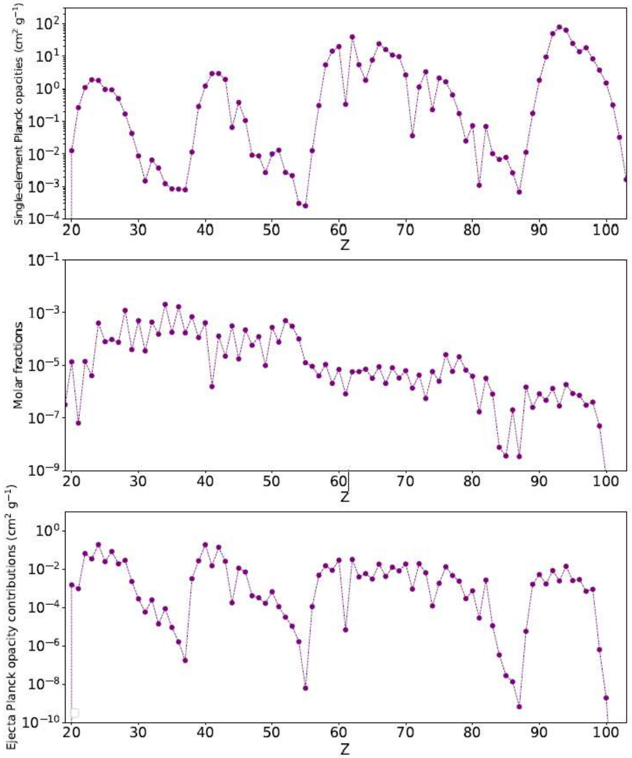


→Single-element Planck mean expansion opacities

→Elemental abundances (molar fractions)

→Contribution of each element to KN ejecta opacity

Main contributors: lanthanides & actinides

+ 3d-shell $Z$≈ 24 + 4d-shell $Z$≈ 40

# Results: NLTE

Forbidden lanthanide lines: example of [Ce III] calculations

| | $\overline{\Delta E/E}$ |
|---|---|
| SR | $0.37 \pm 0.23$ |
| 1VV | $0.17 \pm 0.20$ |
| 2VV | $0.15 \pm 0.20$ |
| 3VV | $0.15 \pm 0.20$ |
| 4VV | $0.15 \pm 0.20$ |
| RCI CC SD $4f + 5p$ | $0.10 \pm 0.11$ |
| RCI CV SrD $4f + 5p$ | $0.10 \pm 0.10$ |
| RCI CV SrD $4f + 5p + 5s$ | $0.05 \pm 0.07$ |
| RCI CV SrD $4f + 5p + 5s + 4d$ | $0.15 \pm 0.10$ |
| RCI Fine-Tuning | $0.003 \pm 0.007$ |
| HFR | $-0.002 \pm 0.007$ |

13 experimental levels belonging to $4f^2$ (NIST)

MCDHF: 4 correlation layers; CC correlation with SD from 4f & 5p ; CV correlation with SrD from 4f, 5p,5s,4d
→Best model: CV with SrD from 4f, 5p,5s + fine-tuning

HFR: $4f^2 + 4f\{6p + 7p + 5f + 6f + 7f\} + 5d^2 + 5d\{6s + 7s + 6d\} + 6d^2 + 6p^2$ and semi-empirical fit

# Results: NLTE

## Example of [Ce III] calculations

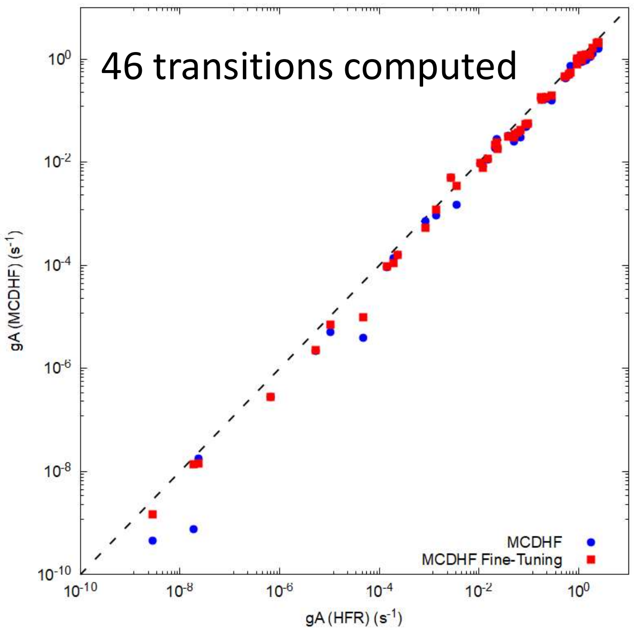


Average relative deviation with HFR for the strongest transition (gA> 0.1 $s^{-1}$): 0.22±0.22 without fine-tuning; 0.15±0.11 with fine-tuning

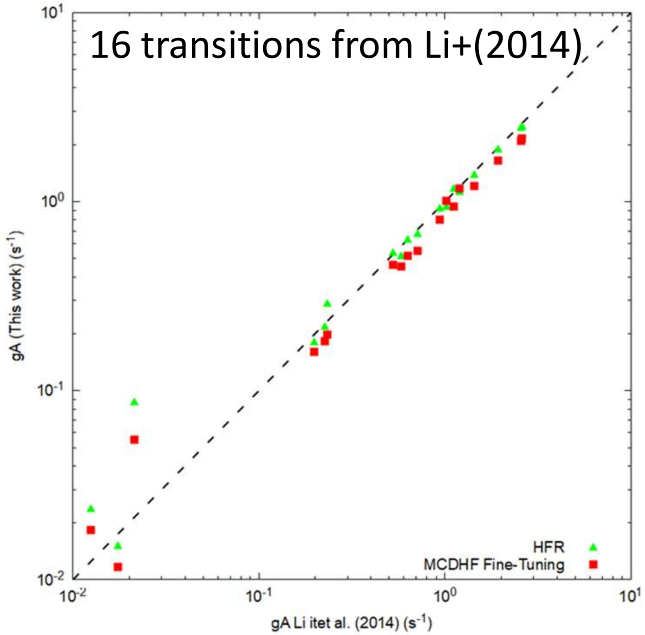


Li+(2014) agree better with HFR

# Results: NLTE

Strongest forbidden transitions (gA>1E-01 s$^{-1}$) overplotted on the +29d and +61 JWST spectra of AT2023vfi (Levan+, 2024;Gillanders & Smart, 2025)

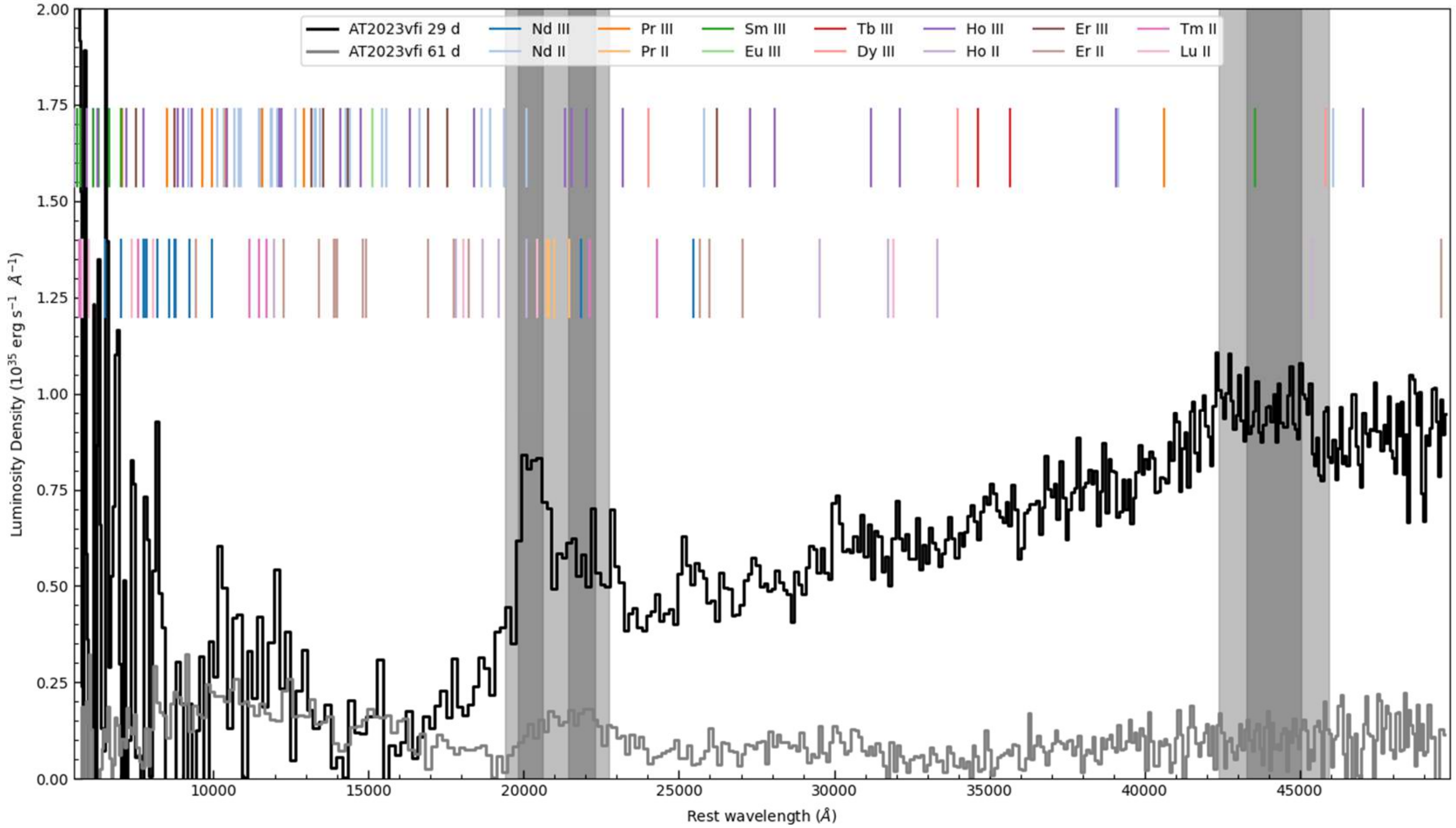


Doppler broadenings:
0.02c (dark grey);
0.04c (light grey)

# Results: NLTE

Strong forbidden transitions between experimentally known levels falling close to the two spectral features observed in AT2023vfi at ~2.1 µm and ~4.4 µm among the >1000 computed

| Spectrum | λ (Å) | Mode | $gA_{HFR}$ ($s^{-1}$) | $gA_{MCHDF}$ ($s^{-1}$) |
|---|---|---|---|---|
| [Ho II] | 20082 | M1 | 3.21E+00 | 3.95E+00 |
| [Lu II] | 20419 | M1 | 1.38E-01 | 1.32E-01 |
| [Pr II] | 20755 | M1 | 2.04E-01 | 2.22E-01 |
| [Pr II] | 20802 | M1 | 1.63E-01 | 1.79E-01 |
| [Pr II] | 20969 | M1 | 1.21E-01 | 1.33E-01 |
| [Pr II] | 21117 | M1 | 1.39E-01 | 1.08E-01 |
| [Ho III] | 21345 | M1 | 9.10E+00 | 3.26E+00 |

| Spectrum | λ (Å) | Mode | $gA_{HFR}$ ($s^{-1}$) | $gA_{MCHDF}$ ($s^{-1}$) |
|---|---|---|---|---|
| [Ho III] | 21540 | M1 | 1.68E+00 | 5.59E+00 |
| [Nd III] | 21855 | M1 | 3.18E-01 | 2.30E-01 |
| [Ho III] | 22031 | M1 | 1.72E+01 | 1.98E+01 |
| [Tm II] | 22137 | M1 | 5.32E+00 | 5.74E+00 |
| [Sm III] | 43563 | M1 | 3.93E+00 | 3.89E+00 |
| [Ho II] | 45396 | M1 | 6.92E-01 | 7.07E-01 |
| [Dy III] | 45828 | M1 | 9.85E+00 | 9.99E+00 |

For more details, see Poster presented by Lucas Maison

# Results: NLTE

Radiative lifetime measurement of the metastable level $4f^6(^7F)5d\ ^8H_{5/2}$ in Sm II
at the DESIREE infrastructure (University of Stockholm)

Decay channels determined with HFR

| Lower Level | E NIST (cm-1) | λ (nm) | $gA_{calc}$ ($s^{-1}$) | Mode |
|---|---|---|---|---|
| $4f^6(^7F)6s\ ^8F_{1/2}$ | 0.00 | 1329.76 | 9.97E-2 | E2 |
| $4f^6(^7F)6s\ ^8F_{3/2}$ | 326.64 | 1379.81 | 2.31E-1 | E2 |
| $4f^6(^7F)6s\ ^8F_{5/2}$ | 838.22 | 1470.51 | 9.20E-2 | E2 |
| $4f^6(^7F)6s\ ^8F_{7/2}$ | 1489.16 | 1613.34 | 9.27E-3 | E2 |
| $4f^6(^7F)6s\ ^6F_{1/2}$ | 1518.29 | 1667.49 | 1.32E-4 | E2 |
| $4f^6(^7F)6s\ ^6F_{3/2}$ | 2003.23 | 1788.91 | 9.47E-4 | E2 |
| $4f^6(^7F)6s\ ^8F_{9/2}$ | 2237.97 | 1831.15 | 1.95E-4 | E2 |
| $4f^6(^7F)6s\ ^6F_{5/2}$ | 2688.69 | 2012.52 | 1.76E-4 | E2 |
| $4f^6(^7F)6s\ ^6F_{7/2}$ | 3499.12 | 2392.51 | 7.88E-6 | E2 |
| $4f^6(^7F)6s\ ^6F_{9/2}$ | 4386.03 | 3085.15 | 7.79E-8 | E2 |
| $4f^6(^7F)5d\ ^8H_{3/2}$ | 7135.06 | 29967.62 | 3.32E-2 | M1 |

**$\tau_{calc}$ = 12.83 s**

Data processing in progress

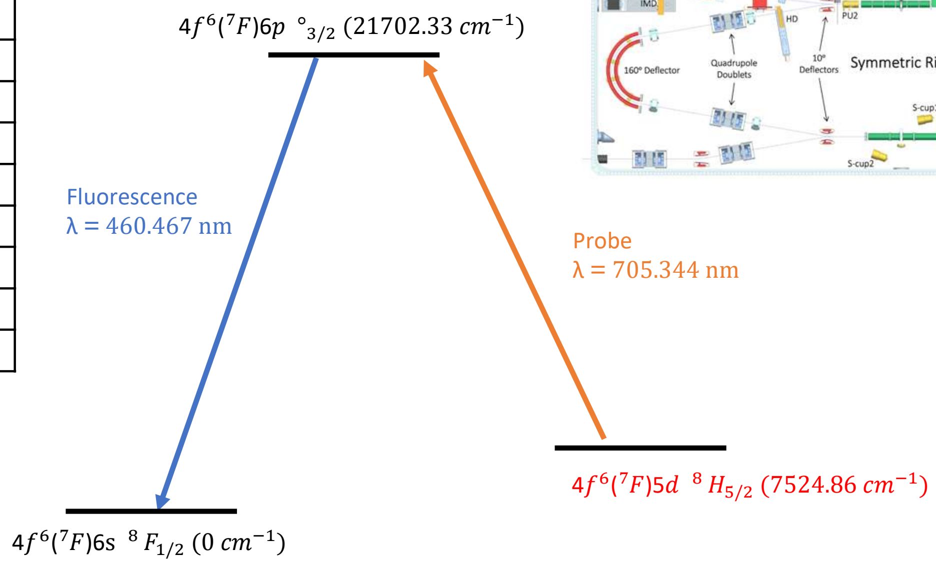


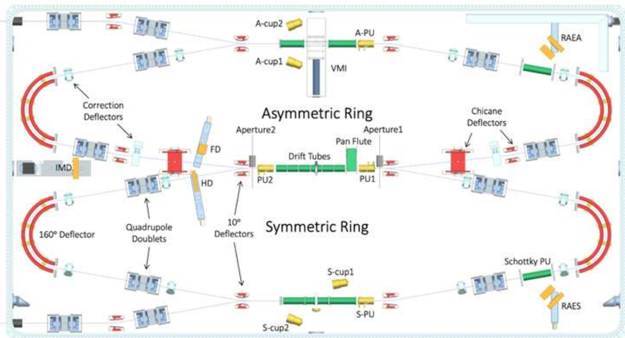

# Results: NLTE

Benchmarking EIE effective collision strengths in Sr II

For more details, see Poster presented by Jérôme Deprince

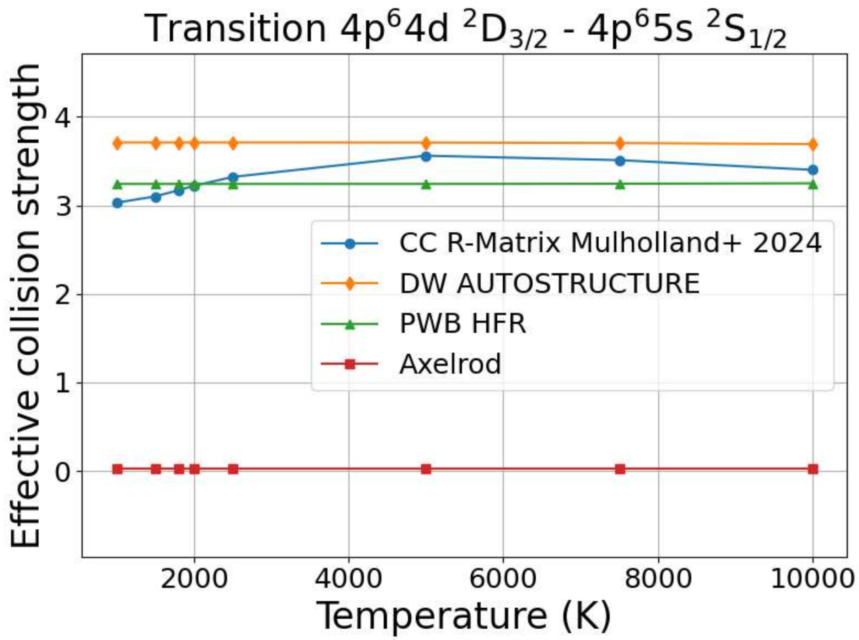


(Deprince & Maison,2026)

→ Order of magnitude correctly reprocuded, outperform Axelrod formula
Balance between feasibility and accuracy to favor completeness

# Conclusions & Prospects

Photosphere phase KN (LTE):

- Large-scale HFR atomic data computations → LTE expansion and line-binned opacities in all heavy elements ($20 \leq Z \leq 103$)
- Focus on lanthanides and actinides (lack of atomic data + dominate KN opacity)
- Atomic data and opacity tables → new database (DOI 10.5281/zenodo.14724537)
- Lanthanides are usually thought to dominate the KN ejecta opacity → actinides + some lighter trans-iron elements as well
- Prospect: improve atomic data for spectral modeling (model complexity, fit to experimental energy levels data when available)

# Conclusions & Prospects

Nebular phase KN (NLTE):

- HFR and MCDHF transition probabilities for >1000 forbidden transitions in Ce-Pr-Nd-Sm-Eu-Tb-Dy-Ho-Er-Tm-Lu III + Nd-Pr-Ho-Er-Lu II → strong M1 transitions predicted close to the AT2023vfi observed features at ~2.1 μm (5 [Pr II], 1 [Ho II], 1 [Lu II], 1 [Tm II], 3 [Ho III], 1 [Nd III]) and at 4.4 μm (1 [Ho II], 1 [Dy III], 1 [Sm III])

- Experimental benchmarking: lifetime measurements in Sm II at DESIREE infrastructure (data processing ongoing)

- PWB and DW EIE effective collision strengths in Sr II -> agree with R-matrix values (within an order of magnitude) → far better than Axelrod and van Regemorter approximations currently used in KN modeling

# Conclusions & Prospects

Nebular phase KN (NLTE):

- Prospect: forbidden lines in other singly and doubly ionized lanthanides ongoing; lifetime measurements (DESIREE proposals submitted for Ce II and Nd II); large-scale EIE collision strength PWB calculations for all elements

# ICAMDATA at Mons (Belgium)

October 26 – 30, 2026

https://icamdata2026.sciencesconf.org/

Registration open very soon !!!

Thank you for your attention!

UMONS

fnrs
LA LIBERTÉ DE CHERCHER

EOS
THE EXCELLENCE OF SCIENCE